Numerical Investigations of Swirling Flow in a Conical Diffuser

Author	Firm / Institution	City, Country	Lecturer (x)
Walter Gyllenram *Håkan Nilsson*	*Division of Thermo and Fluid Dynamics,* *Chalmers University of Technology*	*Göteborg, Sweden*	*X*

Abstract

When a hydraulic power plant is operating at off-design, a swirling flow exits the runner and is convected through the draft tube. The swirling flow gives rise to several features that decrease the efficiency and/or may damage the construction. As a step towards making reliable numerical predictions of the swirling flow in draft tubes, steady computations in an idealised model have been carried out. The model geometry is a straight conical diffuser and O. G. Dahlhaug of NTNU, Trondheim, Norway, has provided experimental data. In this paper, numerical 3D RANS investigations are quantitatively compared to the available experimental data. Good agreement with experimental data was obtained. The discrepancies are partly reminiscent of the nature of the k-ω turbulence model that was used in this work.

Given symmetric geometry and boundary conditions, a fluid flow is most often thought to behave in an equally symmetric manner. If the flow is swirling, this is not generally true. Due to the unstable properties of the symmetric solutions for the averaged Navier-Stokes equations, the flow will collapse into an asymmetric mode. In the first computational cases of this paper, the disturbance that triggers the instability is shown to be imperfections in the CAD-geometry.

Also included is a discussion concerning the development of counter-rotating vortices in the boundary layer of swirling flow in a circular pipe.

Résumé

Quand une centrale hydraulique fonctionne à charge partielle, un écoulement tournant s'échappe de la roue et passe à travers l'aspirateur. Cet écoulement rotatif génère plusieurs effets qui diminuent le rendement et/ou peuvent endommager la construction. Dans le but de rendre fiable les prédictions numériques de l'écoulement tournant, des simulations statiques dans un modèle idéalisé ont été réalisées. La géométrie utilisée est un diffuseur conique droit et les données experimentales ont été fournies par O. G. Dahlhaug de la NTNU de Trondheim en Norvège. Dans cet article, les investigations 3D RANS sont comparées quantitativement aux données expérimentales. Des résultats en accord avec les données experimentales ont été obtenus. Les anomalies sont en partie liées à la nature du modèle de turbulence k-ω qui a été utilisé dans cette étude.

Pour une géométrie symétrique et des conditions initiales données, un écoulement fluide est généralement considéré comme se comportant de manière également symétrique. Si l'écoulement est rotatif, ce comportement n'est généralement plus vérifié. A cause des propriétés instables des solutions symétriques des équations de Navier-Stokes moyénées, l'écoulement va tomber dans un mode asymétrique. Dans le premier cas etudié dans cet article, il est montré que la perturbation qui déclenche cette instabilité est due à des imperfections dans la géométrie du modèle CAO.

Cet article se termine sur une discussion concernant le developpement de vortex contre-rotatifs dans la couche limite de l'écoulement tournant dans un tuyau circulaire.

Keywords

Draft tube, diffuser, swirl, turbulence.

Background

Hydraulic power plants must often run at non-optimal operating conditions (off-design). At an off-design operating condition the water exits the runner with a strong vortical (swirling) flow. When a swirl component of the velocity vector is present, a radial pressure gradient is also observed. If it is strong enough, this can give rise to re-circulation and vortex breakdown (Ref 1) as well as formation of unsteady vortex ropes. The unsteadiness of the vortex can give rise to pressure fluctuations and vibrations that may decrease the efficiency and cause structural damage to the turbine. The efficiency of Kaplan turbine draft tubes is very sensitive to flow separation, which can be triggered by pressure fluctuations. It is very important to be able to give warranties with respect to both efficiency and vibrations/noise that are accurate enough to make reliable economical estimates of the investments. Computations of swirling flow in a simplified model were made as a first step towards making reliable numerical simulations of unsteady effects in a draft tube. Steady solutions of the time-averaged equations have been analysed and validated with experimental data.

Numerical Method

CALC-PMB CFD software was used for the calculations in this work. CALC-PMB has been developed at the Division of Thermo and Fluid Dynamics at Chalmers University of Technology, Göteborg. This in-house code is based on the finite volume method, and the pressure-velocity coupling is solved using the SIMPLEC algorithm. Conformal block structured boundary fitted co-ordinates are used, and the code is designed for parallel computations of three-dimensional flows by domain decomposition. MPI is used for the exchange of information between the different processes/blocks, and two ghost cells are employed at the block interfaces to enable different first and second order difference schemes. The principal unknowns are the Cartesian velocity vector components (U, V, W) and the pressure (P). To avoid spatial oscillations of the pressure field over the collocated (non-staggered) grid arrangement, Rhie & Chow interpolation is applied for convection through the cell faces. See (Ref 2) for further details. The geometry and the computational grids were generated in the ICEM CFD/CAE commercial software and the Ensight commercial software was employed for post-processing.

The Computational Domain

The computational domain is based on the geometry used by O. G. Dahlhaug for the experiments on swirling flow through a diffuser he conducted as a part of his Ph.D. thesis (Ref 3). Figure 1 shows the geometry and the computed main flow pattern.

Figure 1 Streamlines and inlet pressure distribution where the dark colour represents low pressure. Particles are released along a radial line at a fixed tangential position at the inlet and are traced along the steady flow.

The conical diffuser has an area ratio of 2.25, with a half-angle of 3 degrees. Velocity profiles were analysed at three different sections, the inlet, halfway through the expansion and after the expansion. Experimental data were available for validation at the inlet and after the expansion. The geometry was captured by an O-grid formation.

Three Cases

Three cases for different grids and Reynolds numbers were set up. The cases are described in table 1.

Table 1 Three different testcases.

CASE	Re	Sw	Model	Gridsize
1	*280,000*	*0.3*	*High-Re*	*100,000*
2	*2,800,000*	*0.3*	*High-Re*	*100,000*
3	*280,000*	*0.3*	*Low-Re*	*781,250*

The inlet boundary conditions for the mean velocities were linearly interpolated from the measured data provided by Dahlhaug (Ref 3). Neumann boundary conditions were used at the outlet, and kinematic and viscous boundary conditions were employed at the walls. Due to the lack of measured data on turbulent kinetic energy in the free vortex and near wall region, standard boundary conditions for non-swirling pipe flow were used for the turbulent quantities. The *van Leer* (second order) difference scheme was used. Wilcoxes' k-ω

turbulence model (Ref 4) was employed in each case due to its good reputation and robustness.

Coarse grids designed for wall functions were used in cases 1 and 2. The first interior nodes were placed in an assumed log-layer at $y^+ \in$ (30,100). For case 3 the boundary layer was completely resolved, i.e. a low-Re model was used. When using the low-Re model the first node was placed at a wall distance corresponding to $y^+<5$. A posteriori verifications of these criteria have been made.

Results

The computational results are compared with experimental data and the flow is visualised in order to show its structure. All 3D visualisations are made from data obtained from case 3. The results yield an asymmetric flow although a symmetric solution might be expected. The reason for this is explained below.

Vortex Structures and Boundary Layer Interaction

A good way of visualising a vortex structure is to use the scalar obtained from the projection of the vorticity vector on the velocity vector, i.e. the helicity. Here it is also normalised to obtain values in the range of (-1,1) only. A value of 1 represents total alignment of the vectors and negative values means that the vorticity and velocity vectors are pointing in opposite directions. Figure 2 shows that the largest normalised helicity values of are found around the central vortex. Due to the alignment of the mean flow and the negative y-axis, the sign of helicity will be negative for a counter-clockwise swirling of the flow field around a streamwise axis. Figure 3 shows that positive helicity is found in two particular tubes just at the end of the expansion, where the vorticity in the streamline direction changes sign. The reversed vorticity tubes are a necessary condition for the asymmetry of the central vortex. The topology of the counter-rotating vortices has some similarities with the Taylor vortices found in Couette flow (Ref 5).

Figure 2 Iso-surface of normalised helicity at a level of -0.8.

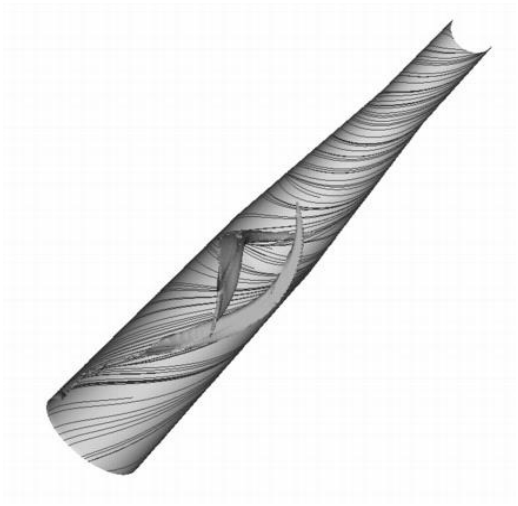

Figure 3 Iso-surfaces of normalised helicity at a level of 0.2, with streamlines passing through the surfaces. The positive iso-surfaces fit perfectly inside the two valleys of the negative iso-surface in figure 2.

Figure 4 Two different iso-pressure surfaces and one streamline, along with planes of pressure distribution where dark grey denotes low pressure.

Figure 4 describes the topology of two iso-surfaces of pressure. An obvious asymmetry develops, starting halfway through the expansion. Figure 5 shows that the boundary layers have a very complex behaviour. The flow resembles features observed experimentally by Spohn et al. (Ref 6) and numerically by Sotiropoulos and Ventikos (Ref 7), who investigated symmetry-breaking in confined swirling flow. A positive radial velocity, and consequently a thinner boundary layer, will be found at the diverging smearlines. The wall shear will be greater due to a higher velocity gradient. The opposite situation is found at the converging streamlines. When wall functions were used, the asymmetries of the smearlines were also present but less evident.

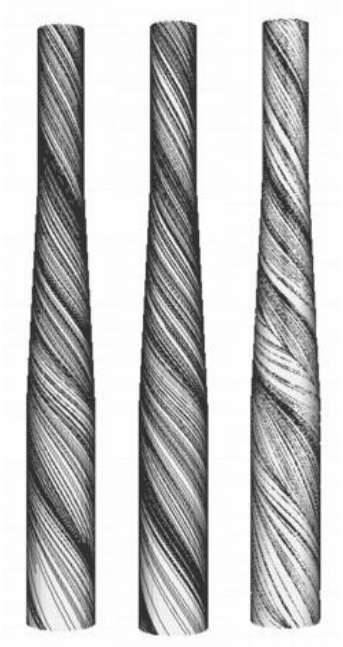

Figure 5 Smearlines for cases 1, 2 and 3 respectively. The use of wall functions and a coarser mesh in case 1 and 2 makes the irregular structures less evident.

Pressure Distribution

As the pressure rises through the diffuser there is a strong decay of the radial gradient, see figure 6. The discrepancy between the cases is obvious during the expansion. The calculations over coarse grids probably suffer from numerical diffusion, smoothing the radial pressure gradient. The pressure rise coefficients are compared in table 2. The two cases most suitable for comparison are cases 1 and 3, due to their common Reynolds number. The difference between the C_p values is about 2.6%.

Table 2 The pressure rise coefficients.

CASE	C_p	Re
1	*0.5937*	*280,000*
2	*0.5737*	*2,800,000*
3	*0.5892*	*280,000*

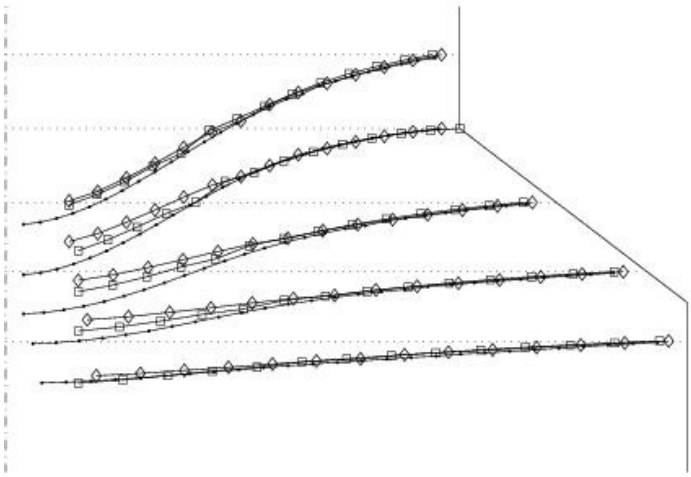

Figure 6 Pressure distribution profiles. The profiles are fixed to zero at the wall in order to make the comparison more convenient. There is a correlation between grid resolution and the relative level of the minimum. Dots: Case 3; Squares: Case 2; Diamonds: Case 1.

The Mean Velocity Profiles

The mean velocity profiles are compared with experimental data in figure 7. The comparisons have been up-scaled in order to show the deviations.

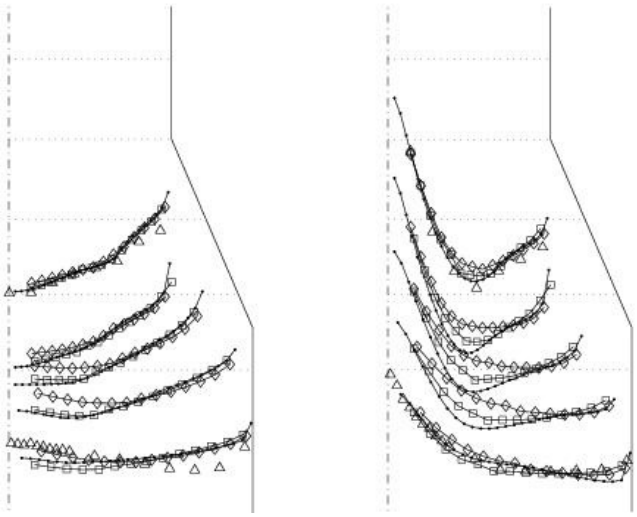

Figure 7 Axial (left) and tangential (right) velocity profiles. Markers: Dots: Case 3; Squares: Case 2; Diamonds: Case 1; Triangles: Experimental data. All computed values are tangentially averaged. The data are scaled to expose the differences. The sample stations are located at the corresponding horizontal dotted lines.

The tangential velocity profiles show similarities with an idealised Rankine vortex. In the centre, the radial gradients are almost constant (forced vortex region) and there are also inflection points corresponding to the free vortex region of a Rankine vortex. What is striking in figure 7 is the discrepancy of the different cases during the expansion, especially for the tangential component. The discrepancy is an obvious indicator of the difficulty of modelling

the flow through the diffuser. At the outlet, the total deviation from experimental data is of the same order for the three calculations: 0.0890, 0.0461 and 0.0750 for cases 1, 2 and 3, respectively. These calculated magnitudes of deviation should not be considered estimates of the computational error. Even though case 2 gives the lowest deviation from experimental data, this is probably a coincidence. The difference in shape of the profiles of case 1 and 3 is a sign of strong grid dependence, and the grid for case 2 must be considered very coarse. The discrepancies between the computed and measured data on axial velocities in the forced vortex region may be explained by the Boussinesq assumption, which is an important part of the turbulence model. In the central, forced vortex region, the radial turbulent mixing will be suppressed. The model will however, predict an isotropic turbulent viscosity and will consequently over-estimate the radial turbulent mixing. Only second derivatives of the velocity profiles will be affected by the error induced by the model. Since the tangential profile in the central region closely resembles a forced vortex and also is an odd function of the radius, the radial second derivative will vanish. Hence, the tangential velocity profile will not suffer from the over-estimation of turbulent mixing.

Instability of the Symmetric Mode

The predominant feature of the visualisations is the asymmetry. Even though solutions for the axi-symmetric (two-dimensional) equations do exist, they will probably never be obtained in a real flow due to the unstable properties of the three-dimensional equations/physics, i. e. the singularity at $r = 0$. Still, there must be something to trigger the instability. Sotiropoulos and Ventikos (Ref 7) suggest that the asymmetry observed in a confined container flow is the result of outer disturbances from small but finite imperfections of a non-ideal environment.

By a series of additional test cases, where the computational grid was rotated and re-projected on the geometry, the symmetry-breaking disturbance in cases 1-3 turned out to be the geometry itself (see (Ref 8) for details). After analysing the radius obtained from the CAD software, a symmetry error of 0.9% was found. The irregularities must be avoided by careful adjustment of the tolerances of the CAD-software. The symmetry-error of the experimental equipment is not available.

Asymmetry of swirling flow in a pipe – Case 4

A simulation of swirling flow in a circular pipe (i.e. the upstream part of the earlier described diffuser) using a less dissipative turbulence model, the Smagorinsky subgrid model, also yielded asymmetric solutions, see figure 8. In this case, the symmetry-error of the geometry was less than 0.01%, and it is not yet clear what triggers the breaking of symmetry. The inlet boundary conditions were here also interpolated from measured data provided by O. G. Dahlhaug. In this case the inlet swirl-factor (Sw) was 0.35. In the pipe, the swirl is rotating in the opposite direction from the diffuser earlier described, and the main vortex therefore carries positive helicity. Negative vorticity will be created everywhere in the boundary layer, i.e. in the free vortex region. What is interesting is how the negative vorticity is clustered in four well-defined vortex tubes, in the form of two double helices. In this case, due to a higher swirl factor than in the earlier described diffuser, the counter-rotating vortices are clearer.

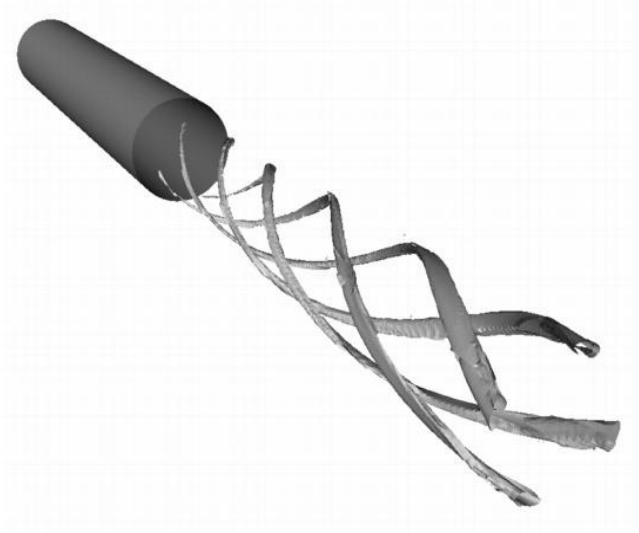

Figure 8 Case 4 – flow through a circular pipe. Iso-surfaces of normalised helicity at a level of -0.9. The tubes can be regarded as vortices swirling in a direction opposite to the main swirl.

Conclusions

The swirling flow in a conical diffuser is very complex and the converging/diverging smearlines along the walls reveal a high level of secondary flow during the expansion. Counter-rotating vortex structures are found at the diffuser exit. The asymmetric behaviour is caused by instabilities in the axi-symmetric mode, and the (dominant) disturbance that triggers the instability in cases 1-3 of the calculations of the flow in a conical diffuser is imperfections in the CAD geometry. In case 4, the calculations of the swirling flow in a pipe, the asymmetry is present even in an 'almost perfect' environment. The symmetry-breaking disturbance has not yet been deduced in this case. The discrepancies regarding the agreements with experimental data are partly reminiscent of the nature of the turbulence model, which over-estimates radial turbulent mixing in the forced vortex region. There is experimental and theoretical evidence of a high level of anisotropy in swirling flow, which cannot be accurately predicted with the standard k-ω model that was chosen for the simulations.

Future Work

Further investigations of swirling flow in diffusers are needed. Different swirl numbers must be considered, as must also the influence of a bending geometry, which to a higher extent would resemble the shape of a draft tube. To examine the anisotropic properties of the large-scale turbulent motions, these must be computationally resolved using LES and unsteady (turbulent) inlet boundary conditions. This will give detailed information on unsteady behaviour not obtainable by RANS modelling. Especially the unsteady behaviour of the central vortex rope will be the subject of future research.

References

Ref 1 Faler, J. H. and Leibovich, S., "An experimental map of the internal structure of a vortex breakdown", *Journal of Fluid Mechanics, Vol. 86, 2:313-335*, 1978.

Ref 2 Nilsson, H., "Numerical Investigations of Turbulent Flow in Water Turbines", Ph.D. thesis, Division of Thermo and Fluid Dynamics, Chalmers University of Technology, Göteborg, Sweden, 2002.

Ref 3 Dahlhaug, O. G., "A study of swirl flow in draft tubes", Ph.D. thesis 1997:30, Institutt for termisk energi og vannkraft, NTNU Trondheim, Norway, 1997.

Ref 4 Wilcox, D. C., "Reassessment of the Scale-Determining Equation for Advanced Turbulence Models", AIAA J., Vol. 26, no. 11, 1299-1310, 1988.

Ref 5 Panton, R. L., "Incompressible Flow", John Wiley & Sons Inc., New York NY, USA, 1996.

Ref 6 Spohn, A., Mory, M. and Hopfinger, E. J., "Experiments on vortex breakdown in a confined flow generated by a rotating disc", Journal of Fluid Mech., Vol. 98, 73-99, 1998.

Ref 7 Sotiropoulos, F. and Ventikos, Y., "The three-dimensional structure of confined swirling flows with vortex breakdown", Journal of Fluid Mech., Vol. 426, 155-175, 2000.

Ref 8 Gyllenram, W., "Modeling of Swirling Flow in a Conical Diffuser", Diploma Work, Division of Thermo and Fluid Dynamics, Chalmers University of Technology, Göteborg, Sweden, 2003